Journal of Cancer and Clinical Oncology

Research Article

Biochemical Characterization of Lung Cancer Tissue: A Spectroscopic Investigation

Mehrotra R[1*], Ray B[1] and Chaturvedi H[2]

[1]Quantum Phenomena and Applications, CSIR-National Physical Laboratory, Dr. K. S. Krishnan Marg, New Delhi, India
[2]Department of Surgical Oncology, Max Super Speciality Hospital, New Delhi, India

***Corresponding Author:** Dr. Mehrotra R, Quantum Phenomena and Applications, CSIR-National Physical Laboratory, Dr. K. S. Krishnan Marg, New Delhi, India; Tel: 91-11-45608315; Fax: 91-11-45609310; E-mail: ranjana@nplindia.org

Published: August 15, 2016

Abstract:
Lung cancer is one of the leading cancer with poor survival rate worldwide. The present investigation is dedicated to biochemical characterization of lung tissues (cancerous as well as normal) using a vibrational spectroscopic approach and thereby, defining infrared markers, which can be utilized to discriminate cancerous lung tissue from its normal counterpart. Post-surgical histopathological tissues (eight cases) were obtained from normal and cancerous sections of a lung tissue microarray. Infrared spectra of eight cases of lung cancer patients of different age groups (45 years to 72 years, 6 male and two female) with different grades of malignancy were acquired using Varian 660-IR spectrophotometer in transmission mode. Significant spectral differences were observed in the molecular signatures of proteins, nucleic acid, lipids and carbohydrates. Absorbance intensity ratios of particular spectral regions have been determined, which further provides detailed insight into pathological state of a cell/tissue. The obtained results may add a part in comprehending structural changes in a cell/tissue and may provide basis to ensure the applicability of this method as an alternative screening approach, when combined with multivariate analysis.

Keywords: Cancer Diagnosis; Infrared Marker; Lung Cancer; Vibrational Spectroscopy

Abbreviations: CT Scan: Computed Tomography Scan; DTGS: Deuterated Triglycine Sulphate; MRI Scan: Magnetic Resonance Imaging Scan; NSCLC: Non-Small Cell Lung Cancer; PET Scan: Positron Emission Tomography Scan; SCLC: Small Cell Lung Cancer; WHO: World Health Organization;

Introduction: Cancer, one of the most severe disease, is estimated as the second leading cause of death in human beings after cardiovascular diseases. Every year, around 8.2 million deaths and 14 million new cases of cancer are reported worldwide, as quoted by World Health Organization (WHO) in 2012 [1]. Amongst these, Lung cancer tops the list with 1.59 million deaths per year, where female lung cancer rates set to rise rapidly. It can be categorized into non-small cell lung cancer (NSCLC) and small cell lung cancer (SCLC). NSCLC, which accounts for 80% of lung cancers, further includes squamous cell carcinoma or epidermoid carcinoma, adenocarcinoma, bronchioalveolar carcinoma, large-cell undifferentiated carcinoma [2]. Extensive research has been reported on lung cancer biology, from its causes (understanding its origin), diagnosis, prevention and cure to treatment, in order to combat this disease. The patients diagnosed with lung cancer, are generally found to be above 60 years of age, as it takes several years to grow and to reach symptomatic stage, when only, the sufferer decides to seek medical help [2]. At early stages, it is asymptomatic and very difficult to detect. Lung cancer is conventionally diagnosed by several imaging techniques such as chest X-rays, bronchoscopy, computed tomography (CT) scan, positron emission tomography (PET) scan and magnetic resonance imaging (MRI) scan [3]. In addition, blood septum cytology and biopsy of cancerous lesion also provide important information regarding tumor location and other affected organs [4]. Although, these screening methods are commonly involved in clinical practice and confirms its (tumor) presence, yet they are limited by identifying cancer at an advanced stage, where it is very difficult to cure it. Lung cancer patients generally have poor survival rate, as it depends upon the stage at which they have been diagnosed.

Hence, the desire to develop a method with more precision, to reduce patient trauma, time delay and high medical costs involved, has inspired researchers to explore a variety of minimally invasive optical imaging and spectroscopy techniques, especially with the ability to distinguish benign lesions from malignant ones [5-8] to improve lung cancer detection. Further, current investigations to establish possible alternative approaches as leading screening tools in cancer therapeutics [9-11] can also enhance the cure percentage of the disease.

Vibrational spectroscopy offers possibility to overcome the limitations of currently employed methods of cancer diagnosis [12,13]. From past few decades, infrared spectroscopy has emerged as potent non-destructive technique in the identification and characterization of various biomolecular and organic components/mixtures both qualitatively and quantitatively. It is suitable for solid, liquid and gaseous samples with nominal sample preparation. Using specific features derived from infrared spectra, the physico-chemical changes present in cells/tissues can be delved [14,15]. Recently, several studies on infrared and Raman spectroscopy, both in near and mid-infrared regions have reported molecular and biochemical alterations in the pre-malignant and malignant cells/tissues from their normal state [16-18]. These evidences when coupled with some algorithms and statistical modeling, can discriminate between cancer tissue and normal tissues of different types of cancer [19,20]. Further, infrared spectroscopy has been involved in the analysis of lung A549 cancer stem cells [21], breast cancer using peripheral blood mononuclear cells [22] and anastomosis tissue based colorectal cancer [23]. Besides this, investigations based on label-free cancer grading in colon [24] and lung cancer [8] identification using infrared spectral histopathology are also possible.

In the present work, the capability of infrared spectroscopy has been utilized to identify the characteristic molecular signatures of lung tissue, as it imparts detailed structural and conformational information of biomolecules [25]. Since, malignant state is associated with changes in cellular biochemistry, we probed alterations in vibrational spectral features of lung cancer tissue, as compared to normal tissue. The information obtained from this study can be instrumental in discriminating lung cancer tissue from normal tissue at molecular level.

Materials and Methods:

Tissue sampling: A total of 16 tissue specimens (eight normal and eight cancerous) from lung cancer patients (eight cases) with clinically suspicious lesions or histologically confirmed malignancy were obtained from Oncology (Cancer Care), Max Healthcare, New Delhi. All the tissue specimens were of grade II and grade III stage. Post-surgical cancer tissue and normal tissue (2-3 cm away from the tumor) samples were collected. For each sample, two tissue sections were cut, one was put on the glass slide for histological review and the other part of the tissue was frozen (-28ºC) to obtain cryostat sections (2-4 µm thick). The cryostat tissue sections were placed on the ZnSe plates without any fixative and used for spectral analysis.

Spectral measurements: The infrared spectra of cancerous and normal lung tissues were recorded on Varian 660-IR spectrophotometer equipped with deuterated triglycinesulphate (DTGS) detector and KBr beam splitter in the transmission mode. Ambient humidity of 45% RH was maintained during the entire experiment. Background spectrum was also collected before recording each spectrum in order to nullify atmospheric (CO_2) interferences. Three infrared spectra were acquired at three different locations (per sample) in the mid-infrared region 4000-700cm^{-1} with a resolution of 4 cm^{-1}and then averaged. A total of 256 scans were collected for each spectrum to improve the signal to noise ratio. Further, the spectra were ratioed against the background spectrum. Prior to analysis, the raw spectra were processed and visualized using Unscrambler 6.0 software, where they were linear baseline corrected and mean normalized. Second order derivative spectra were also determined after smoothening using Savitzky-Golay algorithm with eleven points. The representative infrared spectra were illustrated in figures [both normal (solid line) as well as cancerous (dotted line)].

Results and Discussion:

Analysis of spectral peak variations: The infrared spectra in the mid-infrared (mid-IR) frequency region 4000 cm^{-1} to 700 cm^{-1} (Figure 1), is generated using Varian 660-IR spectrophotometer in order to establish potent biochemical differences between eight cancerous and their corresponding eight normal (control) lung tissue samples. Significant spectral changes in terms of shift in the wavenumber and intensity have been observed for cancerous and normal lung tissue, which may define possible changes in the biomolecular functional groups and their functionality in diseased state. The assignment of spectral features is in accordance to the literature [25-27].

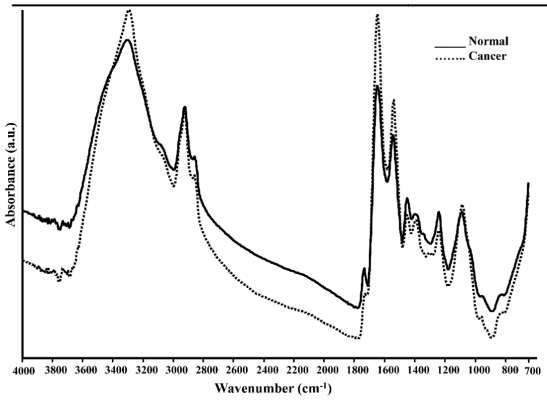

Figure 1: Overlaid Infrared Spectra of Normal and Malignant Lung Tissue in the Region 4000-700 cm^{-1}

Figure 2a represents the overlaid spectra of cancerous and normal lung tissue in the frequency region 1300 cm^{-1}-700 cm^{-1}. The major absorbance peaks observed in the above mentioned region are characteristic to vibrations accredited to nucleic acid content of a cell [26]. In the spectrum of normal tissue, the two major bands attributed to symmetric and anti-symmetric stretching vibrations of phosphodiester groups are visible at 1099 cm^{-1} and 1253 cm^{-1} respectively [26,27]. Cancerous tissue shows a peak of lower intensity with a shift of 8 cm^{-1} from 1099 cm^{-1} to 1091 cm^{-1} for symmetric stretching vibrations of phosphodiester groups, when compared to its normal counterpart. Similarly, the band at 1253 cm^{-1} related to anti-symmetric vibrations of phosphate is shifted to 1244 cm^{-1} with increase in intensity. Additionally, an infrared band corresponding to symmetric stretching vibrations of phosphate monoester group (of phosphorylated proteins) is observed at 950 cm^{-1} [26,28,29] in normal tissue, which is shifted to 959 cm^{-1} and appears as small shoulder peak in cancer tissue. This can be related to structural alterations in nucleic acid under cancerous condition and plays an important role as an internal marker in DNA measurement assays [30].

Further, second order derivative spectra in the 1300 cm^{-1}-700 cm^{-1} region (Figure 2b) is generated to monitor the changes in terms of band shifts and intensity variations, which may enhance the accuracy of our analysis. Therefore, the spectral changes visible from infrared bands (corresponding to nucleic acid content), it can be concluded that the nucleic acid distribution is relatively increased in case of malignancy, which can be related to never ending replication of DNA in a cancerous cell. Similar spectral features have been observed in case of brain [31], ovary [32] and bladder tumors [33].

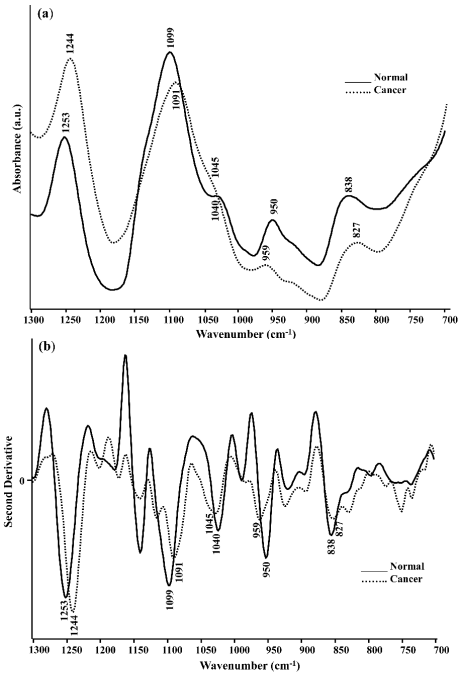

Figure 2: (a) Overlaid Infrared Spectra of Normal and Malignant Lung Tissue; (b) Second Order Derivative Infrared Spectra of Normal and Malignant Lung Tissue in the Region 1300-700 cm^{-1}

Figure 3a shows the infrared spectra of cancerous and normal lung tissue in the region 1800-1300 cm^{-1} and possess key regions in vibrational bands, where significant differences can be seen between the two. This region is characteristic of functional groups associated with protein content of a cell and represents vibrational modes due to amide I, II and III groups [25,26]. This region is highly prone to the changes corresponding to molecular geometry and hydrogen bonds present in the peptides. A prominent intense band at 1652 cm^{-1} (amide I) is attributed to C=O stretching vibrations of amide group in the protein backbone and also represents secondary structure (alpha helix) of proteins [25]. Similarly, the band at 1546 cm^{-1} (amide II) arises due to N-H bending vibrations and is characterized by beta sheet secondary structure of protein [25]. Spectral shifts together with increase in intensity are visible for these two bands in the cancerous tissue [34,35], which have been observed for different kinds of cancer including breast tissues of human [36]. Besides this, two vibrational bands due to in-plane symmetric and anti-symmetric bending vibrations of CH_3 (methyl group of protein) is clearly visible at 1402 cm^{-1} and 1455 cm^{-1} [25,34] in the infrared spectra of normal tissue. These bands show negligible shifts along with intensity deviations in cancerous tissue. Further, spectral changes can be more evident through second order derivative spectra of the above mentioned region (Figure 3b) for both cancerous and normal tissues.

As proteins are linked with most of the physiological processes of a living cell and regulates major metabolic activities in the form of enzymes and hormones. Therefore, monitoring structural changes in the bands related to protein content can give a glimpse of a physiological state of a cell in normal as well as in diseased (cancerous) condition and also provide information on energy related changes to meet the increased energy demands of a cancerous cell [37].

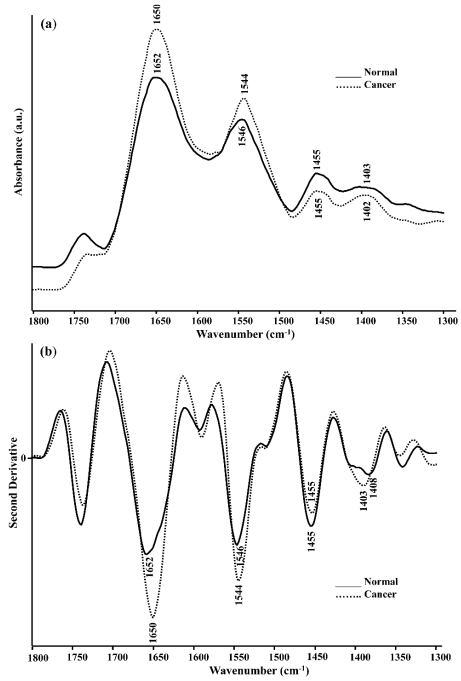

Figure 3: (a) Overlaid Infrared Spectra of Normal and Malignant Lung Tissue; (b) Second Order Derivative Infrared Spectra of Normal and Malignant Lung Tissue in the Region 1800-1300 cm^{-1}

Figure 4a illustrates the overlaid infrared spectra of cancerous and normal lung tissues in the region 3100-2700 cm^{-1}. This region corresponds to stretching vibrations due to lipid hydrocarbons. Spectral changes in terms of intensity are observed in this region for cancerous tissue, when compared to its normal counterpart. The peaks at 2861 cm^{-1} and 2925 cm^{-1} in this region are mainly due to stretching vibrations of the CH_2 and CH_3 groups in acyl chains of lipids [25,27]. The cancerous tissue shows an increase in intensity of the bands, which is more evident in the second order derivative spectra of cancerous and normal tissue in the region 3100-2700 cm^{-1} (Figure 4b). A rapidly multiplying cancerous cell has different metabolic activities and impending requirements of nutrients and energy for the biosynthesis of all the biological macromolecules [38]. From these deviations, it can be inferred that lipid content is increased in the cancerous cells, which is in corroboration with the previous findings of our previous studies, where significant deviations in intensity have been observed for lipid content in ovarian cancerous tissue [32]. Further, these variations can be correlated with cholesterol-rich lipid rafts, which regulate various cellular functions including cell survival and also with the lipogenesis rate that is found to be highly upregulated in fast growing cancer cells [39,40].

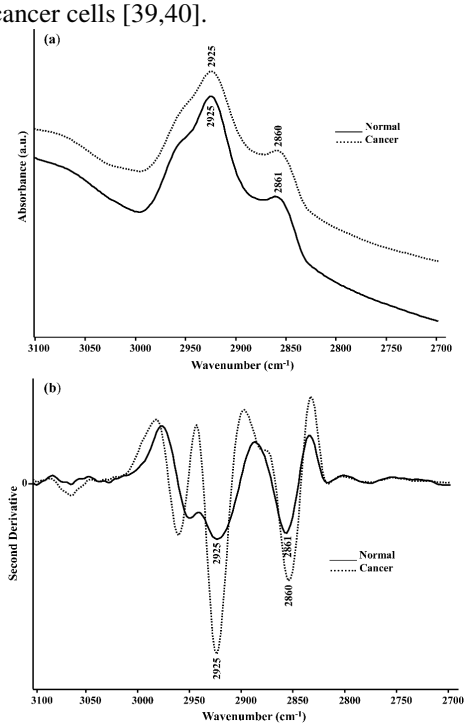

Figure 4: (a) Overlaid Infrared Spectra of Normal and Malignant Lung Tissue; (b) Second Order Derivative Infrared Spectra of Normal and Malignant Lung Tissue in the Region 3100-2700 cm^{-1}

Analysis of absorbance ratios: To discriminate between cancerous and normal lung tissues, different relative intensities of particular spectral regions can be utilized, which may provide the pathological state of a cell or tissue. For this purpose, absorbance ratios of certain wavenumbers accredited to various functional groups of biomolecules have been determined. The assignment of infrared spectral wavenumbers and relative intensity ratios of the eight patient cases under investigation is represented in Table 1. The ratio of absorbance between Amide I and Amide II (1652 cm^{-1}/1546 cm^{-1}) derived from C=O and N-H stretching vibrations of amide groups is found to be increased in case of malignant tissue [14,41,42]. It suggests changes in the secondary structure of protein and also represent structural variations in the proteins' alpha and beta helix as a result of their cancerous transformation. This is in agreement with the results reported by lee and his co-researchers [29], where Amide I and amide II bands for lung cancer cells originated from epithelium are intensified as compared to their normal counterparts.

Further, our results are in corroboration with the findings of Yamada *et al.*[41]. According to their study, the beta sheet content is found to increase as compared to alpha helix content of protein in the necrotic carcinoma condition. In analogy to their study, our results follow a similar pattern.

	Assignment of Infrared Bands		Patient Cases							
			01	02	03	04	05	06	07	08
Relative Intensity Ratio	Amide I/ Amide II (1652 cm^{-1}/1546 cm^{-1})	Normal	1.08	1.01	.03	1.06	1.02	1.01	1.08	1.04
		Cancer	1.12	1.05	1.09	1.11	1.07	1.08	1.12	1.09
	Lipid/Amide I (2861 cm^{-1}/1652 cm^{-1})	Normal	0.89	0.96	0.99	1.01	0.97	0.98	1.06	1.02
		Cancer	0.80	0.87	0.92	0.93	0.89	0.91	0.94	0.95
	Amide I/Collagen (1652 cm^{-1}/1252 cm^{-1})	Normal	1.25	0.99	1.14	1.18	1.09	1.11	1.22	1.16
		Cancer	1.38	1.13	1.28	1.31	1.23	1.27	1.36	1.30
	CH_2/ CH_3 [acyl chain of lipids] (2861 cm^{-1}/2925 cm^{-1})	Normal	1.06	1.02	1.03	0.99	1.01	1.04	1.06	0.98
		Cancer	1.04	1.01	1.00	0.96	0.97	0.99	1.02	0.96
	Glycogen/Amide II (1045 cm^{-1}/1546 cm^{-1})	Normal	0.83	1.02	0.98	1.08	1.06	0.87	0.96	1.01
		Cancer	0.80	0.91	0.91	0.99	0.97	0.81	0.89	0.96
	PO_2^-/Amide II (1099 cm^{-1}/1546 cm^{-1})	Normal	0.88	1.05	1.02	1.12	1.08	0.89	0.98	1.02
		Cancer	0.83	0.93	0.94	1.03	0.99	0.84	0.91	0.95

Table 1: Assignment of Infrared Spectral Wave Number and Relative Intensity Ratios of the Eight Patient Cases Under Investigation in Order to Discriminate Between Cancerous and Normal Cell/Tissue

Further, Lipid/Amide I ratio (2861 cm^{-1}/1652 cm^{-1}) is decreased in case of cancerous tissue as compared to normal. There are several reports, which suggest that lipid-to-protein ratio can be utilized as an infrared marker to differentiate between cancerous and normal state of a cell. It can be helpful in defining different grades of malignancy as well [43,44]. As cancerous cell replicate innumerably very fast and consume more energy, therefore, the reduction in the intensity ratio can be related with the amount of lipid in a cell. The role of lipids in a fast growing cancerous cell and the changes associated with its content ratio is still an intensive subject of research. The absorbance ratio between 1652 cm^{-1} and 1252 cm^{-1} provides the information on the relative content of collagen and is generally increased with different grades of malignancy. Cells, generally have disturbed extracellular matrix (ECM), when they are under malignant stress [45]. It has been reported that stromal collagen concentration encourages the initiation of mammary tumor and its progression in the bi-transgenic mouse tumor model [45]. This ratio increases in case of cancerous lung tissue as compared to normal one. The relative intensity ratio between 2861 cm^{-1} and 2925 cm^{-1}(CH_2/CH_3) due to stretching vibrations of methyl groups respectively, is decreased in case of cancerous condition and provides us information on the deviations in the distribution of lipids and proteins in a cancerous tissue [34]. The reason could be that in a cancer cell, the increased amount of lipids undergo auto-oxidation and results in oxide products of cholesterol, which is also responsible for structural conversion of alpha helix content into beta sheet structure [41]. The infrared region 1100-1000 cm^{-1} is a glycogen rich region, which gives an estimate of carbohydrate content in a cell and the peaks originated in this region are due to the functional groups associated with the cellular molecules [46]. Therefore, analysis of relative intensity ratio of this region band can be crucial in describing the biochemical state of cancerous cell with different grades. The ratio between 1045 cm^{-1} and 1546 cm^{-1} (Glycogen/Amide II) is found to be reduced in lung cancer tissue as compared to its normal counterpart. It has been reported that the carbohydrate levels are generally allied with the progression of disease and its metabolism and absorption is disturbed in the cancerous condition of advanced stage [47]. In order to have an idea about distribution of proteins and nucleic acid content in the cancerous as well as in normal lung tissue, the ratio between 1099 cm^{-1} and 1546 cm^{-1} (PO_2^-/Amide II) has been determined, which is found to be decreased in the cancerous tissue as compared to normal one signifying that the above mentioned content ratio is also disturbed in the diseased state [48].

Conclusion: The present investigation exploits the potential of vibrational (infrared) spectroscopy to probe the biochemical alterations (in a cell/tissue), allied to the cancerous state (diseased) of a cell/tissue and compared with the spectral features of its normal counterpart. The spectral deviations in terms of change in intensity and shift in wavenumber, have been observed in vibrational signatures of lipids, proteins, nucleic acid and carbohydrate. The spectral characteristics of symmetric and anti-symmetric phosphodiester bands (1090 cm^{-1} and 1253 cm^{-1}) assessed major shifts in their position along with intensity variations, whereas bands owing to amide I (1652 cm^{-1}, C=O stretching vibrations) and amide II (1546 cm^{-1}, N-H bending vibrations) revealed minor shifts in the position as well as in intensity, in the cancerous lung tissues.

Further, the bands attributed to acyl chains of lipids (2861 cm^{-1} and 2925 cm^{-1}) represent large intensity changes in cancerous state. The intensity changes are further supported by second order derivative spectral and relative intensity ratio analysis. Nevertheless, we could investigate eight cases, the biochemical features drawn from this study, may unveil the molecular changes associated with the diseased state, which can be the basis of future studies related to the development of spectroscopy based screening tools of the disease. Further, statistical and multivariate analysis with comparatively greater number of lung cancer samples will be performed to ensure the robustness and applicability of this method as non-invasive alternative approach to screen lung cancer with more specificity.

References:

1. Cancer (2015) Facts sheet. World Health Organization (WHO).
2. Sun S, Schiller JH, Gazdar AF (2007) Lung cancer in never smokers - a different disease. Nat Rev Cancer 7: 778-790.
3. Sutedja G (2003) New techniques for early detection of lung cancer. Eur Respir J Suppl 21: 57s-66s.
4. Bach PB, Kelley MJ, Tate RC, McCrory DC (2003) Screening for lung cancer: a review of the current literature. Chest 123: 72S-82S.
5. Müller MG, Valdez TA, Georgakoudi I, Backman V, Fuentes C, et al. (2003) Spectroscopic detection and evaluation of morphologic and biochemical changes in early human oral carcinoma. Cancer 97: 1681-1692.
6. Jess PR, Smith DD, Mazilu M, Dholakia, Riches AC, et al. (2007) Early detection of cervical neoplasia by Raman spectroscopy. Int J Cancer 121: 2723-2728.
7. Mahmood U, Weissleder R (2003) Near-infrared optical imaging of proteases in cancer. Mol Cancer Ther 2: 489-496.
8. Bird B, Miljković MS, Remiszewski S, Akalin A, Kon M, et al. (2012) Infrared spectral histopathology (SHP): a novel diagnostic tool for the accurate classification of lung cancer. Lab Invest 92: 1358-1373.
9. Pepe MS, Etzioni R, Feng Z, Potter JD, Thompson ML, et al. (2001) Phases of biomarker development for early detection of cancer. J Natl Cancer Inst 93: 1054-1061.
10. Wulfkuhle JD, Liotta LA, Petricoin (2003) EF Proteomic applications for the early detection of cancer. Nat Rev Cancer 3: 267-275.
11. Rusling JF, Kumar CV, Gutkind JS, Patel V (2010) Measurement of biomarker proteins for point-of-care early detection and monitoring of cancer. Analyst 135: 2496-2511.
12. Dukor RK (2002) Vibrational spectroscopy in the detection of cancer. Handbook of Vibrational Spectroscopy.
13. Akalin A, Mu X, Kon MA, Ergin A, Remiszewski SH, et al. (2015) Classification of malignant and benign tumors of the lung by infrared spectral histopathology (SHP). Lab Invest 95: 406-421.
14. Mehrotra R, Gupta A, Kaushik A, Prakash N, Kandpal H (2007) Infrared spectroscopic analysis of tumor pathology, Indian J Exp Biol 45: 71-76.
15. Stelling AL, Toher D, Uckermann O, Tavkin J, Leipnitz E, et al. Infrared spectroscopic studies of cells and tissues: triple helix proteins as a potential biomarker for tumors. PLoS One 8: e58332.
16. Sahu R, Mordechai S (2005) Fourier transform infrared spectroscopy in cancer detection. Future Oncol 1: 635-647.
17. Lyng FM, Faoláin EO, Conroy J, Meade AD, Knief P, et al. (2007) Vibrational spectroscopy for cervical cancer pathology, from biochemical analysis to diagnostic tool. Exp Mol Pathol 82: 121-129.
18. Großerueschkamp F, Kallenbach-Thieltges A, Behrens T, Brüning T, Altmayer M, et al. (2015) Marker-free automated histopathological annotation of lung tumour subtypes by FTIR imaging. Analyst 140: 2114-2120.
19. Bergholt MS, Zheng W, Lin K, Ho KY, Teh M, et al. (2011) In vivo diagnosis of esophageal cancer using image-guided Raman endoscopy and biomolecular modeling. Technol Cancer Res Treat 10: 103-112.
20. Mu X, Kon M, Ergin A, Remiszewski S, Akalin A, et al. (2015) Statistical analysis of a lung cancer spectral histopathology (SHP) data set. Analyst 140: 2449-2464.
21. Almeida EA, Facchi SP, Martins AF, Nocchi S, Schuquel IT, et al. (2015) Synthesis and characterization of pectin derivative with antitumor property against Caco-2 colon cancer cells. Carbohydr Polym 115: 139-145.

22. Zelig U, Barlev E, Bar O, Gross I, Flomen F, et al. (2015) Early detection of breast cancer using total biochemical analysis of peripheral blood components: a preliminary study. BMC Cancer 15: 1-10.
23. Salman A, Sebbag G, Argov S, Mordechai S, Sahu RK (2015) Early detection of colorectal cancer relapse by infrared spectroscopy in "normal" anastomosis tissue. J Biomed Opt 20: 75007.
24. Kuepper C, Großerueschkamp F, Kallenbach-Thieltges A, Mosig A, Tannapfel A, et al. (2015) Label-free classification of colon cancer grading using infrared spectral histopathology. Faraday discuss 187: 105-118.
25. Movasaghi Z, Rehman S, ur Rehman I (2008) Fourier transform infrared (FTIR) spectroscopy of biological tissues. Appl Spectrosc Rev 43: 134-179.
26. Banyay M, Sarkar M, Gräslund A (2003) A library of IR bands of nucleic acids in solution. Biophys Chem 104: 477-488.
27. Kong R, Reddy RK, Bhargava R (2010) Characterization of tumor progression in engineered tissue using infrared spectroscopic imaging. Analyst 135: 1569-1578.
28. Lewis PD, Lewis KE, Ghosal R, Bayliss S, Lloyd AJ, et al. (2010) Evaluation of FTIR spectroscopy as a diagnostic tool for lung cancer using sputum. BMC Cancer 10: 1-10.
29. Lee SY, Yoon KA, Jang SH, Ganbold EO, Uuriintuya D, et al. (2009) Infrared spectroscopy characterization of normal and lung cancer cells originated from epithelium. J Vet Sci 10: 299-304.
30. Owens GL, Gajjar K, Trevisan J, Fogarty SW, Taylor SE, et al. (2014) Vibrational biospectroscopy coupled with multivariate analysis extracts potentially diagnostic features in blood plasma/serum of ovarian cancer patients. J Biophotonics 7: 200-209.
31. Krafft C, Sobottka SB, Schackert G, Salzer R (2004) Analysis of human brain tissue, brain tumors and tumor cells by infrared spectroscopic mapping. Analyst 129: 921-925.
32. Mehrotra R, Tyagi G, Jangir DK, Dawar R, Gupta N (2010) Analysis of ovarian tumor pathology by Fourier Transform Infrared Spectroscopy. J Ovarian Res 3: 1-6.
33. Gok S, Aydin OZ, Sural YS, Zorlu F, Bayol U, et al. (2016) Bladder cancer diagnosis from bladder wash by Fourier transform infrared spectroscopy as a novel test for tumor recurrence. J Biophotonics 9: 967-975.
34. Bellisola G, Sorio C (2012) Infrared spectroscopy and microscopy in cancer research and diagnosis. Am J Cancer Res 2: 1-21.
35. Sun X, Xu Y, Wu J, Zhang Y, Sun K (2013) Detection of lung cancer tissue by attenuated total reflection–Fourier transform infrared spectroscopy - a pilot study of 60 samples. J Surg Res 179: 33-38.
36. Bitar RA, Martinho Hda S, Tierra-Criollo CJ, Zambelli Ramalho LN, Netto MM, et al. (2006) Biochemical analysis of human breast tissues using Fourier-transform Raman spectroscopy. J Biomed Opt 11: 054001 (1-8).
37. Cazares LH, Adam BL, Ward MD, Nasim S, Schellhammer PF, et al. (2002) Normal, benign, preneoplastic, and malignant prostate cells have distinct protein expression profiles resolved by surface enhanced laser desorption/ionization mass spectrometry. Clin Cancer Res 8: 2541-2552.
38. DeBerardinis RJ, Lum JJ, Hatzivassiliou G, Thompson CB (2008) The biology of cancer: metabolic reprogramming fuels cell growth and proliferation. Cell Metab 7: 11-20.
39. Swinnen JV, Brusselmans K, Verhoeven G (2006) Increased lipogenesis in cancer cells: new players, novel targets. Curr Opin Clin Nutr Metab Care 9: 358-365.
40. Li YC, Park MJ, Ye SK, Kim CW, Kim YN (2006) Elevated levels of cholesterol-rich lipid rafts in cancer cells are correlated with apoptosis sensitivity induced by cholesterol-depleting agents. Am J Pathol 168: 1107-1118.
41. Yamada T, Miyoshi N, Ogawa T, Akao K, Fukuda M, et al. (2002) Observation of molecular changes of a necrotic tissue from a murine carcinoma by Fourier-transform infrared microspectroscopy. Clin Cancer Res 8: 2010-2014.
42. Li QB, Sun XJ, Xu YZ, Yang LM, Zhang YF, et al. (2005) Use of Fourier-transform infrared spectroscopy to rapidly diagnose gastric endoscopic biopsies. World J Gastroenterol 11: 3842-3845.
43. Huang Z, McWilliams A, Lui H, McLean DI, Lam S, et al. (2003) Near-infrared Raman spectroscopy for optical diagnosis of lung cancer. Int J Cancer 107: 1047-1052.

44. Petibois C, Deleris G (2006) Chemical mapping of tumor progression by FT-IR imaging: towards molecular histopathology. Trends Biotechnol 24: 455-462.
45. Provenzano PP, Inman DR, Eliceiri KW, Knittel JG, Yan L, et al. (2008) Collagen density promotes mammary tumor initiation and progression. BMC Med 6: 1-15.
46. Ramesh J, Salman A, Mordechai S, Argov S, Goldstein J, et al. (2001) FTIR microscopic studies on normal, polyp, and malignant human colonic tissues. Subsurface Sensing Technologies and Applications 2: 99-117.
47. Colagar AH, Chaichi MJ, Khadjvand T (2011) Fourier transform infrared microspectroscopy as a diagnostic tool for distinguishing between normal and malignant human gastric tissue. J Biosci 36: 669-677.
48. Podshyvalov A, Sahu RK, Mark S, Kantarovich K, Guterman H, et al. (2005) Distinction of cervical cancer biopsies by use of infrared microspectroscopy and probabilistic neural networks. Appl Opt 44: 3725-3734.